

This is an Open Access document downloaded from ORCA, Cardiff University's institutional repository:<https://orca.cardiff.ac.uk/id/eprint/167750/>

This is the author's version of a work that was submitted to / accepted for publication.

Citation for final published version:

Czyzewski, Pawel, Slefarski, Rafal, Golebiewski, Michal, Alnajideen, Mohammad and Valera Medina, Agustin 2024. Experimental study of CO₂/H₂/NH₃ influence on CH₄ flameless combustion process in semi-industrial furnace. *Energy* 296 , 131014. 10.1016/j.energy.2024.131014

Publishers page: <http://dx.doi.org/10.1016/j.energy.2024.131014>

Please note:

Changes made as a result of publishing processes such as copy-editing, formatting and page numbers may not be reflected in this version. For the definitive version of this publication, please refer to the published source. You are advised to consult the publisher's version if you wish to cite this paper.

This version is being made available in accordance with publisher policies. See <http://orca.cf.ac.uk/policies.html> for usage policies. Copyright and moral rights for publications made available in ORCA are retained by the copyright holders.



Experimental Study of CO₂/H₂/NH₃ Influence on CH₄ Flameless Combustion Process in Semi-Industrial Furnace

Pawel Czyzewski ^{a,*}, Rafal Slefarski ^a, Michal Golebiewski ^a, Mohammad Alnajideen ^b, Agustin Valera-Medina ^b

^a Institute of Thermal Engineering, Poznan University of Technology, 60-965, Poznan, Poland

^b Collage of Physical Sciences and Engineering, Cardiff University, CF24 3AA, Wales, UK

* Corresponding author: pawel.czyzewski@put.poznan.pl

Abstract

A flameless combustion mode was employed in a semi-industrial furnace to investigate the effect of NH₃ on CH₄, which was diluted by CO₂/H₂ combustible mixtures, serving as the primary fuel. Emission characteristics, as well as toxic compounds and temperature distribution maps, were presented for selected fuels. The combustion system was tested at a constant firing rate of 150 kW_{th} and a constant fuel bulk velocity of 85m/s. We investigated the effects of equivalence ratio, fuel composition and volume share of NH₃ in the fuel. It was found that the equivalence ratio and NH₃ amount have the most significant impact on the emission of fuel nitric oxide in the flameless combustion process. The dilution of CH₄ with CO₂ affects the stretch rate, resulting in an increase in CO levels as well as promoting NO level growth. The calculated dimensionless Conversion Factor (CF) shows that the dilution gas, CO₂, significantly impacts the reduction of NH₃ to NO, but only for low-content fuel-bound nitrogen (up to 1%). The lowest values of CF were measured for a high equivalence ratio, corresponding to the typical oxygen content for flameless combustion process.

Keywords: Flameless combustion, CH₄/CO₂/H₂/NH₃, Ammonia combustion, nitric oxide, emissions.

Highlights

- MILD combustion of ammonia fuel blends is studied in semi-industrial combustion chambers
- Impacts of CO₂/H₂ dilution on CH₄-NH₃ fuel were investigated.
- Low oxygen environment led to reduced fuel NO generation.
- CO₂ chemical and thermal effect on NO generation is discussed.

Abbreviations

CF	Conversion Factor
CH ₄	Methane
CO ₂	Carbon dioxide
H ₂	Hydrogen
HiTAC	High Temperature Air Combustion
LHV	Low Heating Value
MILD	Moderate or Intense Low-oxygen Dilution
NH ₃	Ammonia
NO	Nitric Oxide
NO _x	Nitric Oxides
ppm	Parts per million
ppmv	Parts per million by volume

1. Introduction

Nowadays, the efforts to decarbonise the energy sectors are escalating at an unprecedented rate worldwide. As for February 2022, the global warming level was recorded at 1.19 °C [1], mainly due to the rise in the concentration of greenhouse gases in the atmosphere, of which more than 90% are CO₂ released due to human activities. This trend is anticipated to continue to 1.5 °C between 2030 and 2050, and could reach 2.0 °C in 2100 [2], reinforcing the global threat of climate change and global warming. A promising strategy for long-term sustainability currently focuses on steadily decreasing dependence on fossil fuels while gradually increasing the use of renewable energy sources (RES). However, RES present the challenge of periodic electricity surpluses and shortages, which create economic management difficulties. Consequently, research has pivoted towards using alternative energy fuels such as hydrogen (H₂), ammonia (NH₃), and methanol (CH₃OH), as well as developing their corresponding technologies for a near-zero emission economy. [3,4]. Notably, the combustion of these alternative fuels does not necessarily result in the emission of greenhouse gases such as CO₂ and nitrogen oxides [5–7].

The current geopolitical situation in Europe further drives the urgency to significantly reduce the use of imported fossil fuels, principally natural gas. This situation amplifies the growing interest in alternative technologies for producing combustible gases, with a focus on biogas. Biogas is a preferred form of high-calorific gas production and is considered a zero-emission fuel [8]. Furthermore, biogas plants offer a solution to another environmental issue, which is the disposal of organic origin waste. Due to the stability issues with renewable energy power productions [9], initial solutions will likely emphasise fuel flexibility, blending hydrogen and its carriers like ammonia with conventional fuels such as biogas or methane. Most of the existing literature on this topic is still based on laboratory-scale studies and their corresponding numerical results [10]. There is a noticeable lack of research on pilot-scale low- to medium-power systems exceeding 100kW, as well as large industrial capacities measured in megawatts.

1 On the other hand, High-Temperature Air Combustion technology (HiTAC, also known as MILD
2 combustion, flameless combustion or volumetric combustion) [11–13], offers an alternative to
3 conventional combustion techniques. This technology significantly improves process efficiency through
4 the regeneration of exhaust heat and internal exhaust gas recirculation, thereby substantially reducing
5 nitrogen oxide emissions [14]. The technique involves introducing air heated to temperatures exceeding
6 the fuel's auto-ignition temperature, thereby maintaining a low oxygen concentration. This approach has
7 already been successfully implemented in the metallurgical and energy industries [15,16].
8
9
10

11 **1.1 Influence of CO₂ on Combustion**

12
13 Non-combustible CO₂ as well as water vapour recirculating within the combustion chamber have two main
14 effects on the combustion process: alteration of the flow and thermodynamic properties of the mixture,
15 and direct chemical effect of CO₂, including increased energy transport through CO₂ radiation. The most
16 significant thermal influence, particularly in high-temperature combustion, is exerted by tri-atomic CO₂.
17 The heat capacity of CO₂ strongly depends on temperature; unlike two-atom nitrogen, the main component
18 of the gases present in the combustion chamber [17]. The presence of CO₂ in the mixture with methane
19 leads to a reduction in the burning velocity and alters the shape of the flame [18]. Studies on the impact of
20 CO₂ on the structure and emission of turbulent diffusion methane flames [19] have observed a decrease in
21 flame length, temperature and NO_x concentration. In addition, CO₂ significantly reduces the flammability
22 limits. Several studies have been conducted to understand the reasons for these observations. Jia et al. [20]
23 investigated the ignition characteristics of CH₄ mixtures with CO₂ and N₂, concluding that the elementary
24 reaction sequence of the CO→CO₂ pathway is crucial for ignition initiation in highly diluted methane with
25 CO₂. CO₂ in a mixture with CH₄ increases the ignition temperature, mainly due to its high heat capacity.
26
27
28
29
30
31
32
33
34
35
36
37

38 As the proportion of CO₂ in the oxidant increases, the flame becomes elongated [21]. Ignition initiation
39 becomes more challenging as the proportion of CO₂ in the methane mixture increases. In conventional
40 combustion, this necessitates the use of rich mixtures [22]. Guiberti et al. [23] studied the flames of
41 methane mixtures with CO₂ by measuring the chemiluminescence of OH, CH radicals, and CO₂ molecules.
42 They demonstrated that as the proportion of CO₂ increases, the OH/CO₂ ratio decreases.
43
44
45
46
47

48 Numerical calculations carried out by Liu et al. [24] for premixed flames indicate that the chemical effect
49 of CO₂ significantly reduces the burning rate of methane and hydrogen-doped flames. The importance of
50 the CO₂ chemical effect increases with increasing CO₂ concentration in the fresh mixture. The dominant
51 reaction pathway for the chemical effect of CO₂ is the CO₂+H↔CO+OH reaction. The consumption of H
52 radicals by CO₂ plays a major role in inhibiting the rate of combustion (reaction H+O₂↔O+OH). It has
53 been shown that the chemical effect of CO₂ in methane flames is more significant than in hydrogen flames.
54
55
56
57
58
59
60
61
62
63
64
65

1
2
3
4
5
6
7
8
9
10
11
12
13
14
15
16
17
18
19
20
21
22
23
24
25
26
27
28
29
30
31
32
33
34
35
36
37
38
39
40
41
42
43
44
45
46
47
48
49
50
51
52
53
54
55
56
57
58
59
60
61
62
63
64
65

These results were subsequently confirmed in the work of Zhang et al. [25], in which CO₂ and N₂ were added to methane. They performed a numerical analysis of combustion in a 20kW laboratory furnace and calculated the chemical kinetics of the reaction in a well-stirred reactor (WSR). Their study highlighted the difficulties in achieving conditions for appropriate stable flameless combustion when the fuel is diluted with CO₂. The main reason for this is the reduction in combustion temperature and ignition delay caused by the chemical effect of CO₂. The addition of CO₂ enhances CO formation, mainly through the reactions $H+CO_2 \rightarrow OH+CO$ and $CO_2+CH_2 \rightarrow CO+CH_2O$. Zhenjun and Tong [26] analysed the kinetics of the combustion of methane and methane with CO₂. In the combustion of methane, the decomposition of CH₄ to CO occurs in the first step, and the final oxidation of CO to CO₂ takes place in the second step. Thus, the elementary oxidation reactions of carbon monoxide are extremely important for the oxidation of methane. CO₂ is not inert, but actively participates in chemical reactions, mainly through the reactions $CO_2+H \leftrightarrow CO+H_2$ and $O_2+CO \leftrightarrow O+CO_2$. The latter reaction is slow and does not significantly contribute to the formation of CO₂. However, it serves as an initiator of the chain sequence. The actual CO oxidation step ($CO+OH \leftrightarrow CO_2+H$) contributes to the formation of free H atoms.

A study by Colorado et al. [27] investigated the flameless combustion of biogas (60% CH₄ and 40% CO₂) and natural gas in a 50kW furnace. The furnace efficiency remained practically constant for both fuels. In both cases, NO_x and CO emissions were minimal. A slight reduction in temperature was observed when CO₂ was dilution. Interestingly, when biogas was used instead of natural gas, the heat load of the flameless system could be maintained at a constant level. Importantly, despite achieving higher efficiency with the regenerative system., the outlet loss was higher compared to a natural gas-fired burner. When the same amount of gas flows through the flue gas heat regeneration system, the combustion products of biogas have a higher concentration of CO₂, which exhibits better radiation properties, higher absorption capacity and greater heat capacity. These characteristics enhance the heat transfer between the flue gas and the honeycomb regenerators. The utilisation of the flameless mode enables the attainment of a longer and more diffuse reaction zone, a more uniform temperature profile, and improved system efficiency through the use of honeycomb regenerators. However, it should be noted that adding very high proportions of CO₂ to the methane mixture makes the chemical effect of CO₂ influence negligible [28].

1.2 Influence of H₂ on Combustion

The high combustion temperature of H₂, with an adiabatic combustion temperature of 2400K, leads to the intense formation of nitrogen oxides according to a thermal mechanism [29]. Hydrogen flames are also characterised by a high laminar combustion velocity, which is a parameter that defines the reactivity, diffusivity and exothermicity of the combustion reaction [30]. Appropriate management of the combustion process for H₂ fuel can achieve emissions comparable to those of hydrocarbon fuels. To date, various methods have been proposed for the combustion of H₂ [31] and its mixtures with hydrocarbon fuels.

1
2
3
4
5
6
7
8
9
10
11
12
13
14
15
16
17
18
19
20
21
22
23
24
25
26
27
28
29
30
31
32
33
34
35
36
37
38
39
40
41
42
43
44
45
46
47
48
49
50
51
52
53
54
55
56
57
58
59
60
61
62
63
64
65

In the work of Cavigiolo et al. [32], an experimental study of the H₂ combustion with methane demonstrated the possibility of efficient application of flameless mode. Compared to methane burning, additional advantages in terms of emissions were obtained. This was attributed to an increased rate of gaseous fuel delivery into the chamber. The addition of H₂ enabled stable combustion conditions even with less air heating. Celtek et al. [33] conducted numerical investigations of CH₄ and H₂, and their mixtures in an industrial furnace using Ansys software with GriMech 3.0 model [34], and compared the results with the experimental results of Ayoub et al. [35]. A decrease in NO_x emissions was observed with increasing H₂ content, primarily due to a reduction in the intensity of prompt mechanism formation. The numerical analyses demonstrated that the internal recirculation of combustion products affects the shape and composition of the combustion zone by lowering the reaction temperature and rate. Despite CH₄ having a lower combustion temperature compared to its mixtures with H₂, the observed NO_x emissions are higher. This was attributed to a higher amount of OH radicals and the presence of HCN, an intermediate compound in the elementary reactions of NO formation. Although the amount of OH radicals is approximately 20x10³ times higher than that of HCN, the latter is much more efficient in terms of NO_x formation potential. This accounts for the lower emissions from fuels doped with H₂. However, the addition of up to 20% H₂ by volume to methane increases the combustion temperature, resulting in a longer exposure of the O, H, and OH radicals to high temperatures. Together with the aforementioned presence of HCN, this results in the highest emissions among the fuels tested.

Similar observations were made by Ardila et al. [36]. In their experimental study of a 28kW burner, methane was mixed with H₂ (up to 45% of the fuel volume). The increase in the equivalence ratio (ϕ) contributed to lower NO_x emissions. The addition of H₂ increased the stability of the combustion process by reducing pressure fluctuations and enhancing dynamic stability. Despite the high proportion of H₂ in the fuel, NO_x emissions remained very low [36]. This reduction in emissions is due to the decrease in the C/H ratio, which inhibits the increase in NO_x emissions caused by the prompt mechanism.

1.3 Influence of NH₃ on Combustion

Due to its flammability and lack of carbon in its chemical structure, ammonia has the potential to be used for combustion in zero-emission electricity generation systems. The energetic use of ammonia for direct combustion or co-firing with other gases offers several benefits [10], including low energy storage costs. Compared to batteries, the maintenance and construction costs of ammonia infrastructure are comparable to those of traditional fossil fuel-based energy carriers such as natural gas or crude oil. The temperature of ammonia flames is lower compared to hydrocarbon flames. This is attributed to the absence of CO₂ in the combustion products, which is a gas with a high heat capacity, especially at high temperatures in combustion chambers.

1 The laminar combustion velocity of ammonia is significantly lower than that of methane combustion, with
2 a maximum value of 7 cm/s at $\phi=1.1$, compared to 38.2 cm/s for $\phi=1$ [34,37]. The volumetric heat release
3 during ammonia combustion is lower than that of methane. However, the flame thickness is greater due to
4 the slower combustion rate. Nitrogen oxides are mainly generated according to the fuel mechanism, and
5 their highest concentration is found at the flame front, gradually decreasing in the post-flame zone.
6
7

8
9
10 In the kinetics of the reactions leading to nitrogen oxide formation in NH_3 combustion, an excess of OH
11 radicals promotes the conversion of NH_i intermediate radicals to NO. Mendiara and Glarborg [38] observed
12 that the addition of NH_3 to methane flames results in a significant reduction in NO emissions due to the
13 consumption of OH radicals by CO_2 instead of NH_i radicals. CO_2 consumes hydrogen atoms to form CO.
14 The formation of HNO radicals from NH_i , along with OH, H_2 , O, O_2 and H_2O , is crucial in the formation
15 of NO [10]. It has been shown that an increase in OH radicals directly affects the production of NHO,
16 which further leads to NO formation. Therefore, the addition of hydrogen in $\text{NH}_3/\text{H}_2/\text{air}$ flames leads to
17 higher NO_x generation [39]. For ammonia-methane mixtures under rich flame conditions, a positive effect
18 of high proportions of CO_2 in reducing NO was observed. The opposite trend was obtained for lean
19 mixtures. Based on experimental studies in a flow reactor, Mendiara and Glarborg [38] developed a
20 mechanism for the combustion of methane with ammonia, taking into account the effect of CO_2 and N_2 .
21 The high proportion of CO_2 did not affect the initiation of methane oxidation. However, its increasing
22 proportion contributed to an increase in NO levels for rich mixtures and inhibited this increase under
23 stoichiometric and lean mixtures conditions. The high concentration of CO_2 during combustion supports
24 the formation of CO and affects the amount of OH radicals. The authors concluded that the above
25 relationships, rather than direct reactions between N radicals and CO_2 , are responsible for the effect of CO_2
26 on ammonia conversion. In flameless combustion technology, the reaction zone is extended in the chamber
27 volume, which suggests that this will have the effect of weakening the intensity of the fuel mechanism of
28 nitrogen oxide formation and consequently reducing its emissions.
29
30
31
32
33
34
35
36
37
38
39
40
41
42

43 Based on the above considerations, the experimental studies in this paper analysed whether the dependence
44 of the decrease in the intensity of ammonia conversion to nitrogen oxides is relevant for CO_2/H_2 -added
45 mixtures in volumetric combustion. At present, many technologies for the use of H_2 and fuels with a high
46 proportion of H_2 have already reached the stage of technology readiness for implementation or
47 commercialisation [40,41]. However, there are limited studies on the combustion of H_2 mixtures with
48 renewable biogas and ammonia on a pilot and industrial scale. To date, no studies have been carried out
49 on the combustion of biogas and methane-hydrogen mixtures with consideration of the increasing
50 proportion of ammonia in these fuels. In addition, an additional novelty, was the use of a functioning
51 industrial burner so as to test whether it is possible to burn the aforementioned decarbonized gases together
52 with ammonia in existing industrial installations while avoiding high fuel NO emissions.
53
54
55
56
57
58
59
60
61
62
63
64
65

This presumption was achieved, and in the most favorable combustion process configurations the conversion of nitrogen bound in ammonia to NO did not exceed 5% for 5%vol. NH₃ in the fuel. The results presented in this paper, along with its scientific analysis, address the need for pilot studies as a link between experimental research and the implementation of technologies in industrial installations.

A comprehensive analysis of the existing literature indicates a limited number of papers that have presented research results on the combustion of H₂ and ammonia mixtures at high proportions. This highlights a research gap in this area. The research conducted in this paper focused on pilot studies within the power range. These studies serve as valuable preliminary investigations in the field.

2. Methods

2.1 Experimental setup

Experimental investigations were conducted on the combustion process of unconventional gaseous fuels with a significant ammonia content using flameless combustion technology. The experiments were implemented using an industrial combustion system equipped with the Japanese NFK company HRS-Ux-144d4 gas burner as shown in **Fig. 1**. The burner comprises four cyclic heat regenerators that heat the supplied air to a level 50-80K lower than the temperature of the combustion chamber wall. The tests were carried out with three levels of oxygen in the dry flue gas, ranging from 1 to 5%, corresponding to equivalence ratio values between 0.75 and 0.95. The power firing rate was kept constant at 150kW. The combustion chamber had dimensions of 1200mm x1200mm x2700mm and was equipped with a number of measuring points located at 150mm, 650mm, 1150mm, 1650mm and 2150mm from the burner plate. The operating temperatures during the experiments were approximately 1300K for the combustion chamber and 1230 - 1250K for the preheated air. A summary of the combustion process parameters is shown in **TABLE 1**. In order to maintain a constant fuel flow rate, adjustments were made to the burner to facilitate the replacement of nozzles with varying diameters.

TABLE 1: Parameters of the combustion process.

Parameter	Value
Power firing rate [kW]	150
Fuel bulk velocity [m/s]	80-90
Fuel temperature [K]	300
Thermal load of combustion chamber [kW/m ³]	40
Average temperature of combustion chamber [K]	1300-1310
Equivalence ratio [-]	0.75-0.95
Average temperature of combustion air [K]	1230-1250

The investigated fuel gases were supplied to the combustion chamber from a mixer fuelled by a set of high-pressure tanks. The mass flow rates of the gaseous components were controlled using Brooks mass

flow meters. The fuels were preheated to 300K in the water-gas heat exchanger and injected into the combustion chamber through a central nozzle. The bulk velocity for all the examined fuels was maintained at a constant level, ranging from 80 m/s up to 90 m/s.

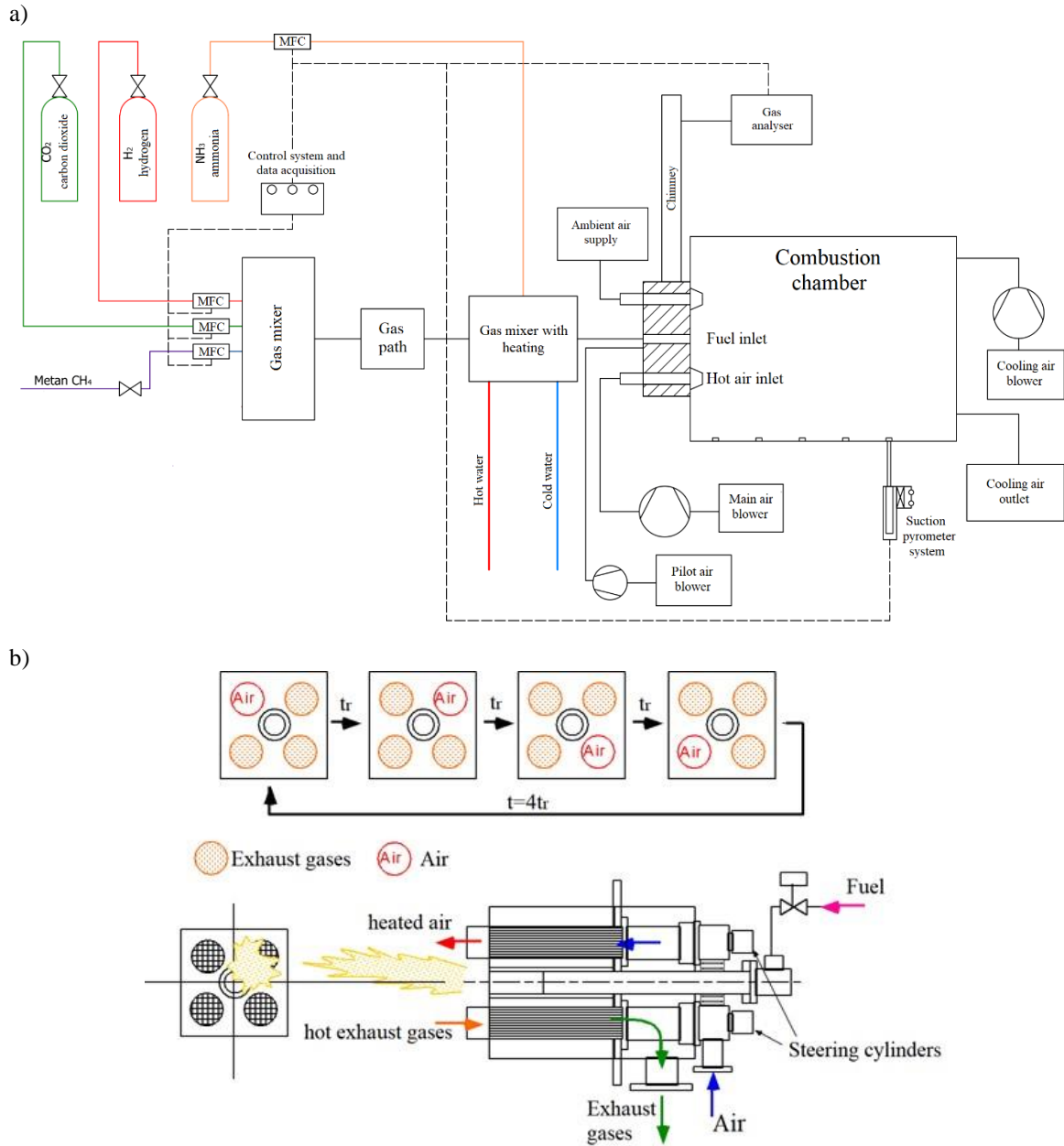


Fig. 1: Schematic diagram of a) the combustion test rig b) burner operation sequence

2.2 Fuel

Tests were conducted on two groups of decarbonised gaseous fuels, which are commonly used in high-temperature thermal processes. These fuels were compared to natural gas, which served as the reference basic fuel. The first fuel group consisted of biogas derived from wastewater treatment and agriculture

biogas plants, with methane contents of 50% and 70%. The second tested fuel was a mixture of methane and hydrogen, which is a Power to X energy carrier (which is a series of techniques and ways to convert, store and use renewable electricity). The hydrogen content in this fuel ranged from 10 to 30% by volume, corresponding to a fuel energy share of 3% to 11%. The fuel samples also contained ammonia, with a concentration of up to 5% volume. The composition of the fuels used in this study is presented in **TABLE 2**. The proportion of ammonia in the supplied fuel was calculated using Equation (1):

$$\frac{x.NH_3}{x.CH_4+x.CO_2+x.H_2} \times 100\% \quad (1)$$

where x is the individual share of each component.

TABLE 2: Fuel composition of fuels studied in this research.

Fuel (%vol)	LHV [MJ/m ³]	NH ₃ [%vol]
M100 (100%CH ₄)	34.8 – 35.9	
BioM70 (70CH ₄ , 30%CO ₂)	24.6 – 25.1	
BioM50 (50CH ₄ , 50%CO ₂)	17.8 – 17.9	0.0 -5.0*
H2M70 (70CH ₄ , 30%H ₂)	27.7 – 28.3	
H2M80 (80CH ₄ , 20%H ₂)	30.0 – 30.9	
H2M90 (90CH ₄ , 10%H ₂)	32.4 – 33.4	

* Ammonia share was calculated according to Eq.1

The influence of the physicochemical properties of gaseous fuels and operating parameters on pollutant emissions, specifically: nitric oxide (NO), carbon monoxide (CO), and slip ammonia (NH₃) was investigated. Emerson NGA 2000 CLD gas analysers, including (CO, CO₂: infrared, NO: chemiluminescence; O₂: paramagnetic) were used to measure the concentrations of NO, CO, CO₂ and O₂ in the flue gases. The slip ammonia was measured using the PIK method. The analyser types and ranges is presented in TABLE 3. To determine the distribution of toxic compounds and temperature within the chamber, a water-cooled suction pyrometer probe equipped with a type S thermocouple was employed. During the tests, all data were collected and recorded at a frequency of 1Hz for 90 seconds and then averaged. The error maintained a consistent value of ~ 1% of the measurement range. This consistent error margin across all tests did not significantly impact the qualitative analysis of the results, as it remained uniform throughout the testing process.

TABLE 3 Types of gas analysers with accuracy data

Name	Range	Accuracy
Analyser CO ₂ Emerson (detekcja IR)	0 - 25%	
O ₂ Emerson Analyser (parameagnetic detection)	0 - 30%	±1% of measuring range
CO Emerson Analyser (IR detection)	0 - 5000 ppm	
NO Emerson Analyser (chemiluminescence detection)	0 - 1000 ppm	

In a study of component and temperature distribution inside the combustion chamber, tests were conducted to examine the effect of maximum considered ammonia volume on the combustion process. Each test was conducted at a constant equivalence ratio of $\phi=0.85$ which was determined to be the most favourable in terms of achieving the lowest possible emissions of nitrogen oxides while maintaining low levels (several ppmv) of carbon monoxide emissions. A summary of the fuels used in the study of toxic substances distribution and temperature is presented in TABLE 4.

TABLE 4 The composition of gaseous fuels used during the diagnosis of the distribution of toxic substances and the temperature inside the combustion chamber.

Fuel name	CH ₄	CO ₂	H ₂	NH ₃ *
	[%vol.]			
	Main fuel			NH ₃
M100	100	0	0	0
M100NH3	100	0	0	5
BioM70NH3	70	30	-	5
BioM50NH3	50	50	-	5
H2M70	70	-	30	0
H2M70NH3	80	-	20	5

* Ammonia share is calculated according to Eq.1

The proportion of inert gases, nitrogen, and CO₂ in the fuel gas leads to additional dilution of the flue gas. In order to accurately quantify the conversion of nitrogen in ammonia molecules to nitric oxides, the emission levels are measured in relation to the amount of dried flue gas. To provide a comprehensive representation of this conversion intensity, a dimensionless conversion factor (CF) [42] is introduced. The CF is calculated Using Equation (2), where n_{NO} represents the number of moles of nitric oxide in the exhaust gas, and n_{NH_3} represents the number of moles of ammonia supplied in the fuel.

$$CF = \frac{n_{NO}[\text{mol}]}{n_{NH_3}[\text{mol}]} \cdot 100\% \quad (2)$$

3. Results and Discussion

The intensity of fuel oxidation within the combustion chamber volume can vary depending on its location. After conducting the emission tests selection of representative fuels was subjected to an extended analysis of their oxidation process. This analysis involved measuring local parameters within the combustion chamber volume, including the level of toxic compounds such as carbon monoxide (CO) and nitric oxide (NO), as well as temperature distribution. The experimental results were presented by showcasing the NO

emission results (recalculated to 0%O₂ reference conditions), CF and distribution of temperature, NO and CO within the combustion chamber.

The emission curves were initially grouped separately based on the proportion of CO₂ and H₂ in the mixture with methane. All tests included an increasing proportion of ammonia, and thus, the main factor influencing the emission characteristics was the share of ammonia in the tested fuel. In addition, the equivalence ratio was varied across three levels: $\phi=0.95$, $\phi=0.85$ and $\phi=0.75$.

3.1 CH₄ + NH₃ Combustion

A base case was established using a mixture of pure methane, along with progressively increasing proportions of ammonia. The results obtained from these tests are presented in **Fig. 2** [43]. The methane test served as reference point for the subsequent analyses of emissions.

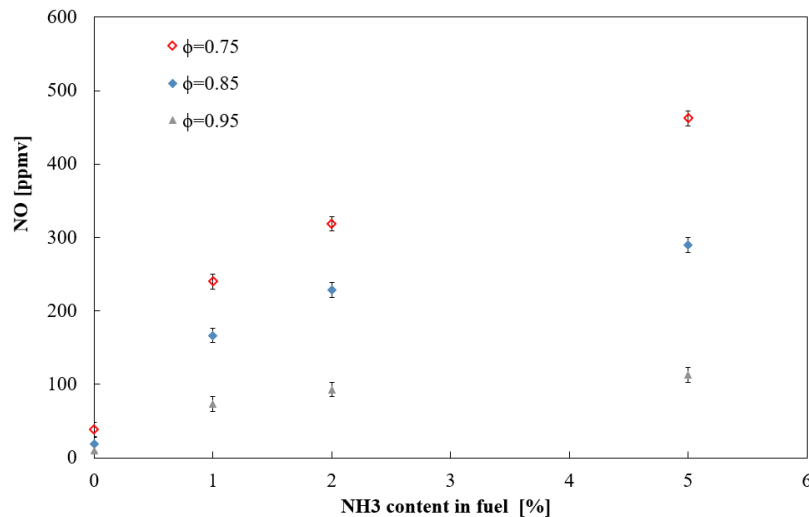


Fig. 2: Molar fractions of nitrogen oxide NO in the flue gas versus f_{NH_3} content in the fuel [43].

The growth dynamics of the molar fraction of NO formation are highest in the range of 0 and 1% of NH₃ content in fuel (by volume). However, as the NH₃ proportion continues to increase, this correlation tends to decrease, particularly for cases with low oxidiser excess ($\phi=0.95$). Increasing of equivalence ratio resulted in the highest NO emissions drop, achieving levels below 10 ppmv and even for cases with 2% and 5% of ammonia did not exceed 100ppmv level (93ppmv) for 5%NH₃ case. At $\phi=0.75$ the emission levels significantly rose and reached nearly 500ppm in case with 5%NH₃ in the fuel. An increase in the NH₃ content in the fuel leads to a decreasing impact on the level of NO formation. The relationship between the conversion factor (CF) of ammonia to nitric oxides is depicted in **Fig. 3**.

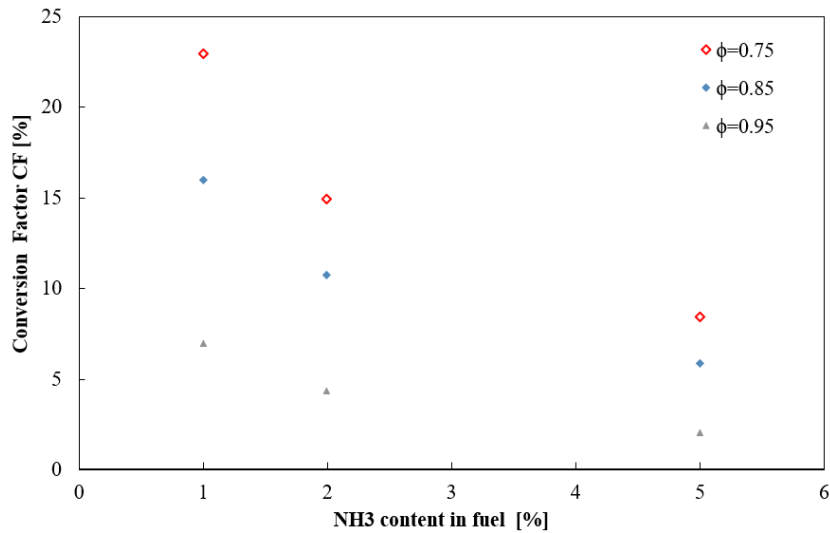


Fig. 3: Conversion factor of NH_3 to nitric oxide versus volume share of ammonia in the fuel.

Similar to the case of emission levels studies for the combustion of methane-ammonia mixtures, the conversion factor of NH_3 to NO strongly depends on the amount of air supplied for combustion. Higher equivalence ratios result in lower intensities of NO formation from NH_3 . In addition, there is a clear dependence of the conversion factor on the proportion of ammonia in the fuel. The greater the amount of fuel, the lower the conversion level. At $\phi=0.95$, only 2% of NH_3 converts to NO . The obtained CF values demonstrate the significant predominance of reactions leading to the conversion of nitrogen bound in ammonia to diatomic nitrogen.

Fig. 4 presents the experimental results of NO , CO and temperature distribution within the chamber for **M100** and **M100NH3** fuels. It can be seen that the area with the highest CO concentration partially corresponds to the region with the highest temperatures, indicating the main regions of fuel oxidation. The remaining space in the test chamber exhibits a very low CO level, similar to the CO emission levels observed in exhaust gases. In the representations of NO distribution, two distinct areas can be identified. One corresponds to NO emissions levels found in exhaust gases, while the other area exhibits very low NO values, not exceeding 16 ppm. Interestingly, this low NO zone coincides with the location of the high CO zone.

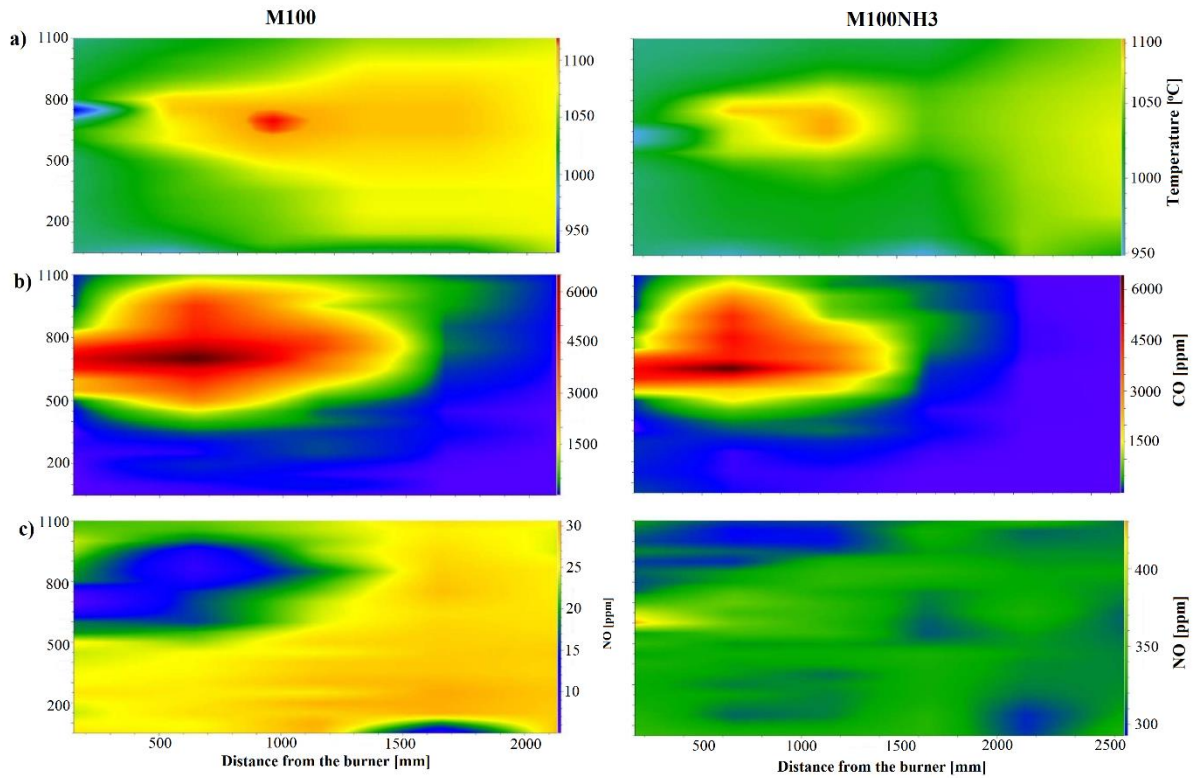


Fig. 4: Distribution of a) temperature b) carbon monoxide c) nitrogen oxide NO for M100 and M100NH3 fuels ($\phi=0.85$).

Introduction of 5% ammonia into the fuel (fuel **M100NH3**) shifted the high-temperature region towards the burner head side. However, only a slight decrease in the maximum temperature value was observed. The addition of ammonia did not have a significant impact on the CO levels within the research chamber.

It can be seen from the results obtained from the NO distribution analysis for **M100NH3** fuels that the major area of NO oxide formation occurred in the fuel inlet area where the lowest temperature was observed. This indicates the fuel mechanism involved in NO formation. The peak of nitric oxide formation was 50% higher than the final emission level, concluding, that some NO is reduced in post-combustion regions.

3.2 CH₄ + CO₂ + NH₃ Combustion

The impact of ammonia on the combustion of methane and CO₂ mixtures was investigated. The effect of increasing molar proportions of ammonia was examined for two different CO₂/CH₄ ratios: 30% and 50% CO₂). The resulting effect on NO_x emission levels is presented in **Fig. 5**.

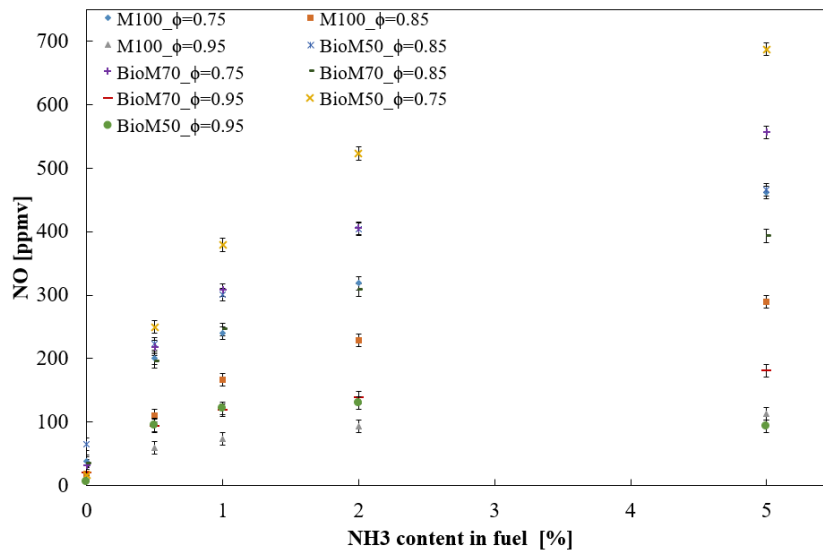


Fig. 5: Share of nitrogen oxide NO in the flue gas depending on the share of ammonia in the fuel supplied for CO₂ added (BioM70, BioM50) fuels.

Similar to the combustion of pure methane with ammonia (fuel M100), the excess of oxidiser has the greatest influence on the intensity of NO formation, and the lowest NO levels were measured at $\phi=0.95$. For a share of ammonia up to 2% by volume, the NO emission levels for BioM50 and BioM30 fuels are practically the same and slightly higher than the NO emissions for the methane-ammonia mixture. However, a different trend was observed for the BioM50 fuel with 5% NH₃ where a slight decrease in NO levels in exhaust gases was observed with an increase in the proportion of NH₃.

The CF of NH₃ to NO for methane- CO₂ mixtures, with an increasing proportion of ammonia in the gaseous fuels (BioM50 and BioM70), is shown in Fig. 6. Compared to M100 ammonia mixed fuels, the CH₄ - CO₂ mixture exhibited lower minimal conversion, which even dropped below 1% for BioM50 fuel. The values of the conversion factor are strongly correlated with the amount of air supplied to the combustion process. It was observed that the higher volume of NH₃ in the fuel, the lower effect of CO₂ content. For all the analysed cases, the CF values did not exceed 8% even for a 5% share of NH₃ in the fuel.

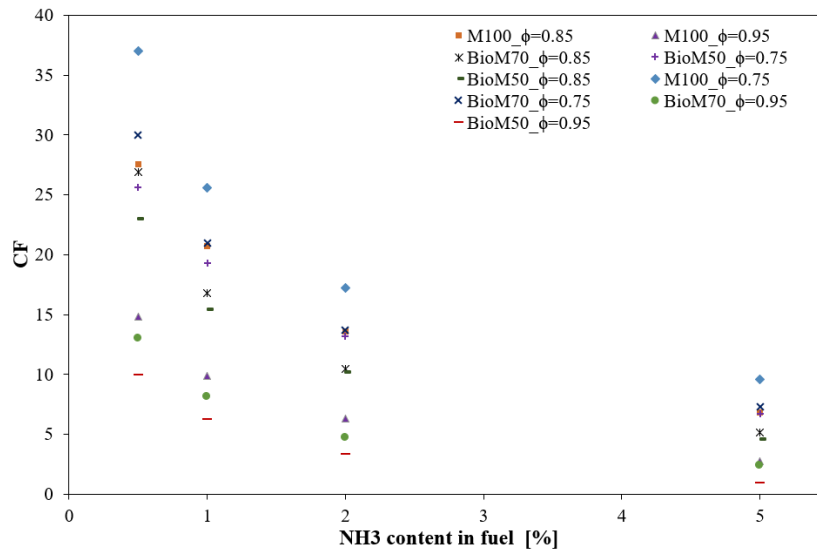


Fig. 6: Conversion factor of ammonia to nitrogen oxide NO for its mixtures of methane and CO₂ depending on the increasing volume share of ammonia in the supplied gaseous fuel.

No significant effect was observed for the 30% share of CO₂ (BioM70) compared to the base fuel (M100). However, as the share of CO₂ was further increased to 50% (BioM50 fuel), a significant increase in the level of NO in the exhaust gas was observed. Specifically, there were 20% and 30% in the NO level for 5% and 1% NH₃, respectively. For an ammonia share of up to 2% by volume of the total fuel supplied, the NO emission levels for CO₂M50 and CO₂M30 fuels are virtually the same (121 and 130 ppm for 1 and 2% NH₃, respectively) and 15 ppm higher than the NO emissions for the methane-ammonia mixture. A different observation from the other characteristics was made for the CO₂M50 fuel for 5% ammonia by volume. With an increase in the proportion of NH₃ in the fuel, there was a decrease in the molar proportion of NO in the exhaust gas from 130 ppm for 2% NH₃ to 93 ppm for 5% NH₃.

As the amount of air supplied for combustion increased at $\phi=0.85$, the proportion of nitrogen oxides in the flue gas increased. There was no significant effect of the 30% share of carbon dioxide (CO₂M70) on NO emissions compared to the base fuel (M100). However, a further increase in the share of CO₂ in the fuel to 50% of the methane/carbon dioxide mixture (CO₂M50 fuel) resulted in a significant increase in the level of nitrogen oxides in the exhaust gas of 20 and 30% for 5 and 1% NH₃, respectively. This indicates that the chemical effect of CO₂ plays a predominant role in NO formation, while the thermal effect is minor. Furthermore, this underlines the importance of the residence time of the reacting gases within the combustion chamber. A deeper understanding of this effect can be gained by examining the distribution of parameters within the combustion chamber. The distributions of temperature, CO and NO for BioM70NH₃ and BioM50NH₃ fuels are presented in Fig. 7.

The most significant difference observed when burning **BioM70NH₃** compared to **M100NH₃** fuel is the change in the location of increased and decreased NO levels zones. The area of increased NO levels

extended up to 1150 mm from the burner wall, with a maximum width of 400 mm. This indicates a change in the reaction kinetics influenced by the thermal/chemical effects of CO₂.

The thermal effect of CO₂ was observed in the fuel injection zone, where a small area of NO decrease was detected. Increasing the share of CO₂ in the methane mixture to 50% (**BioM50NH3** fuel) led to a significant decrease in the temperature inside the test chamber, according to the thermal mechanism.

On the burner side, a narrow area of temperature drop is visible. This means that the heat exchange between the recirculating exhaust gases and the fresh mixture is not sufficient to heat it to temperatures close to the average in the chamber. This results in temperature unevenness inside the chamber. Compared to fuel BioM70NH₃, the highest CO zone extended along the axis of the combustion chamber. The highest levels of NO were observed in the boundary areas. In the central part of the chamber, near the lowest temperature, an elongated narrow zone of NO reduction was observed. This implies that for the combustion of ammonia in a mixture of methane and CO₂, fuel nitrogen oxides are formed with the greatest intensity, not in the main reaction zone, but in the area of recirculating flue gases. The thermal effect of CO₂ addition, as well as the reduction of the reaction rate, reduces NO formation in the fuel-rich zone.

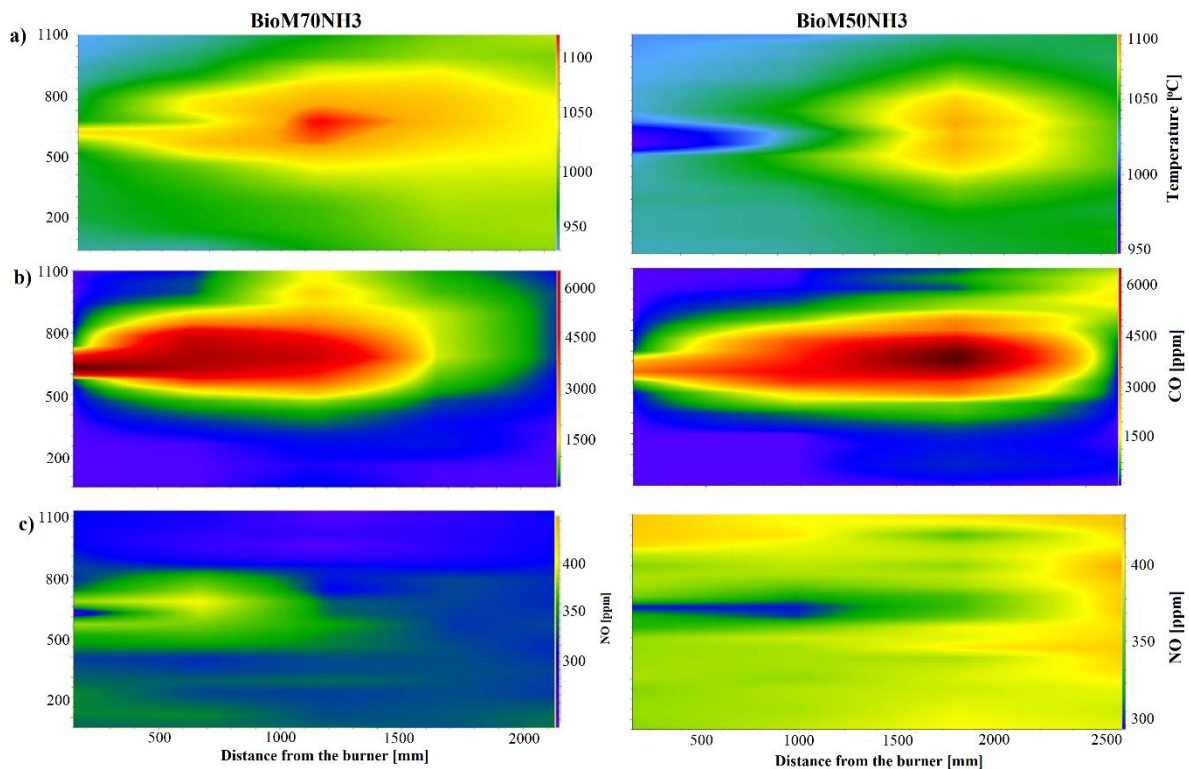


Fig. 7: Distribution of a) temperature b) carbon monoxide c) nitrogen oxide NO for BioM70NH₃ and BioM50NH₃ fuels ($\phi=0.85$).

3.3 CH₄ + H₂ + NH₃ Combustion

The next stage of this study involved investigating the impact of H₂ on emission, the location of the heat release zones, and the formation of toxic compounds. **Fig. 8** presents selected characteristics of the effect

of increasing molar proportions of ammonia for three H₂/CH₄ blends (10%, 20% and 30% of H₂) on NO level. A higher proportion of H₂ in the fuel resulted in slightly higher nitrogen oxide emissions, particularly in the case where 30% of H₂ was present in the fuel. This trend was observed across all levels of equivalence ratios that were tested. For 1% of NH₃ vol. in the fuel increase from 240 to 275ppmv at $\phi=0.75$. Even sharper increase from 73 to 115ppmv at 0.95. Similar tendency was observed for 5% NH₃ in the fuel. At $\phi=0.75$ NO increased from 462 to 473, while at $\phi=0.95$ from 112 to 181ppmv. It indicates that the rise of NO emission is more prominent for higher equivalence ratios.

The analysis of the conversion factor for CH₄/H₂/NH₃ fuels (**Fig. 9**) confirms the trend observed in the examination of emission characteristics (**Fig. 8**). As the proportion of ammonia in the supplied fuel increases, its conversion to nitrogen oxides decreases. The most favourable conversion factor values were observed at $\phi=0.95$. However, at low shares of NH₃ in the fuel (1% and 2% by volume of the fuel), the CF is significantly higher. This means that the increase in NO generation resulting from a higher volume of NH₃ in the fuel contributes to the intensification of the reduction of NH₃ to NO through the NH₂→NNH→N₂, NH→N₂O→N₂, and N→H schemes [44]. It can be concluded that the increase in the number of OH radicals in the reaction zone formed from the H₂ oxidation process did not noticeably affect the value of CF.

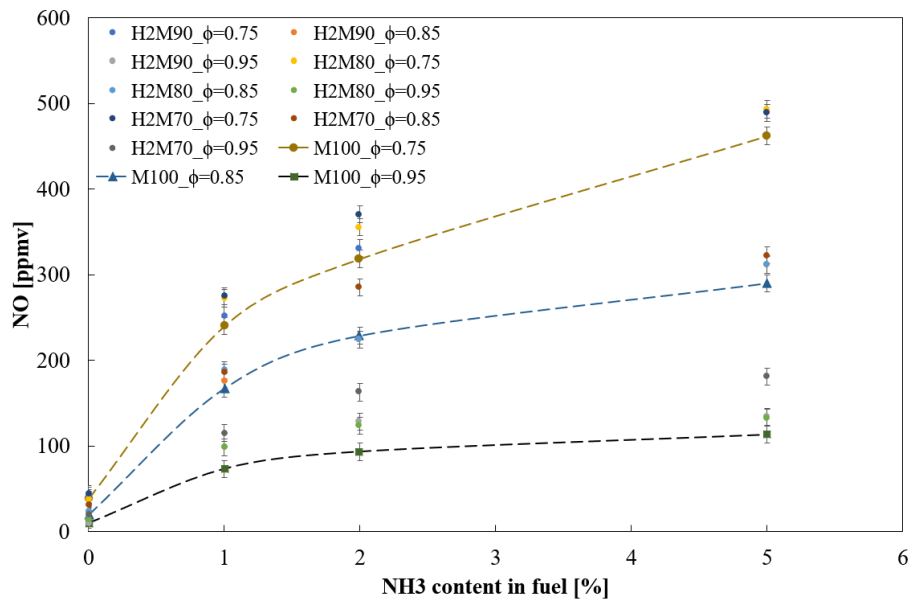


Fig. 8: Share of nitrogen oxide NO in the flue gas depending on the share of ammonia in the fuel supplied for methane as the main fuel CH₄.

The distribution tests were conducted separately to examine the impact of H₂ in a mixture with methane (**H2M70**), and subsequently, the addition of ammonia to the stream of supplied fuel gas (**H2M70NH3**). The results of these investigations are presented in **Fig. 10**. In comparison to the base case (**M100**), a noticeable shift of the high-temperature zone towards the burner plate is observed.

1 In addition, an increased temperature was observed in the area of the fuel nozzle outlet, indicating partial
2 combustion and the initiation of main heat release in that zone. Compared to M100 fuel, the average
3 temperature in the burner wall zone is lower, except for the fuel injection zone. This slight temperature
4 decrease inside the chamber may be attributed to the higher rate of hydrogen combustion compared to
5 methane, as well as the change in the composition of the recirculating exhaust gas. The recirculating
6 exhaust gas primarily consists of water vapour, which has a lower CO₂ content compared to the M100 fuel.
7
8 Since CO₂ has the highest specific heat among the considered exhaust gas components, its reduced
9 presence in the recirculating reaction products leads to a diminished temperature gradient during heat
10 transfer between the combustion products and reacting species.
11
12
13
14
15
16
17
18
19
20
21
22
23
24
25
26
27
28
29
30
31
32
33
34
35
36
37
38
39
40
41
42
43
44
45
46
47
48
49
50
51
52
53
54
55
56
57
58
59
60
61
62
63
64
65

1
2
3
4
5
6
7
8
9
10
11
12
13
14
15
16
17
18
19
20
21
22
23
24
25
26
27
28
29
30
31
32
33
34
35
36
37
38
39
40
41
42
43
44
45
46
47
48
49
50
51
52
53
54
55
56
57
58
59
60
61
62
63
64
65

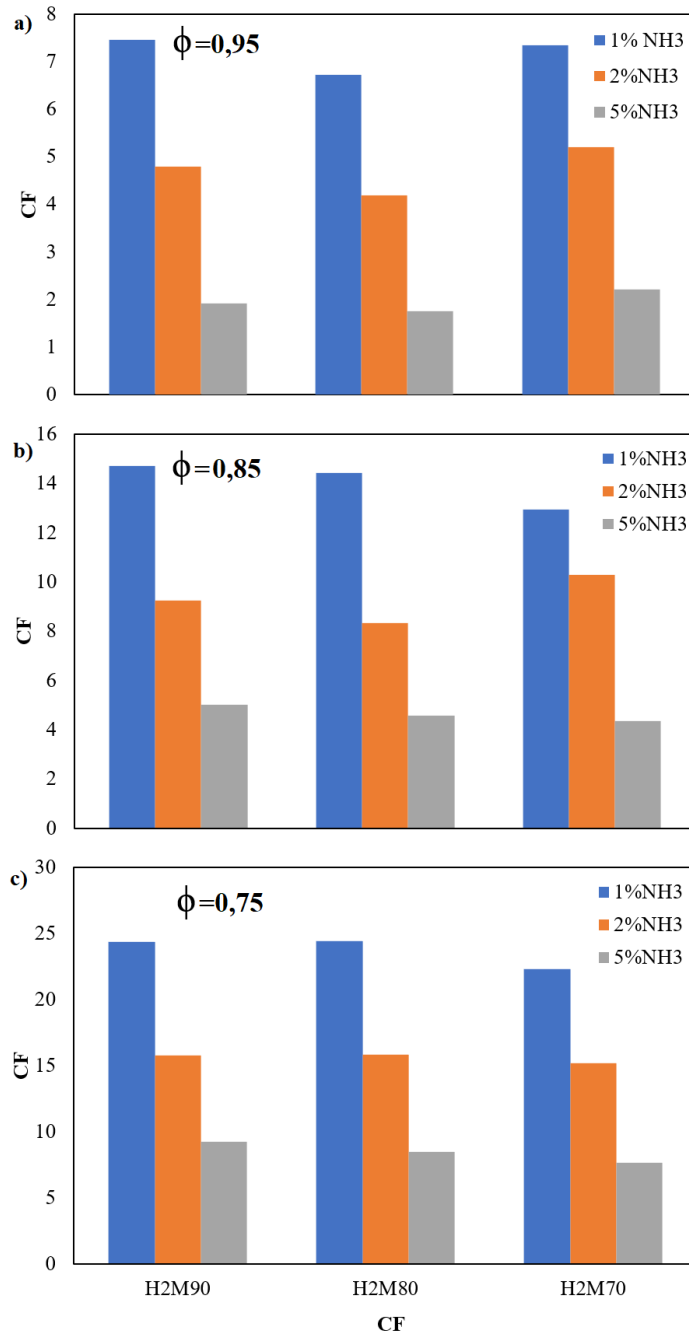


Fig. 9: Conversion factor of ammonia to nitrogen oxide NO for its mixtures of methane and hydrogen for different volume shares of ammonia in the supplied gaseous fuel; a) $\phi=0.95$, $\phi=0.85$, $\phi=0.75$.

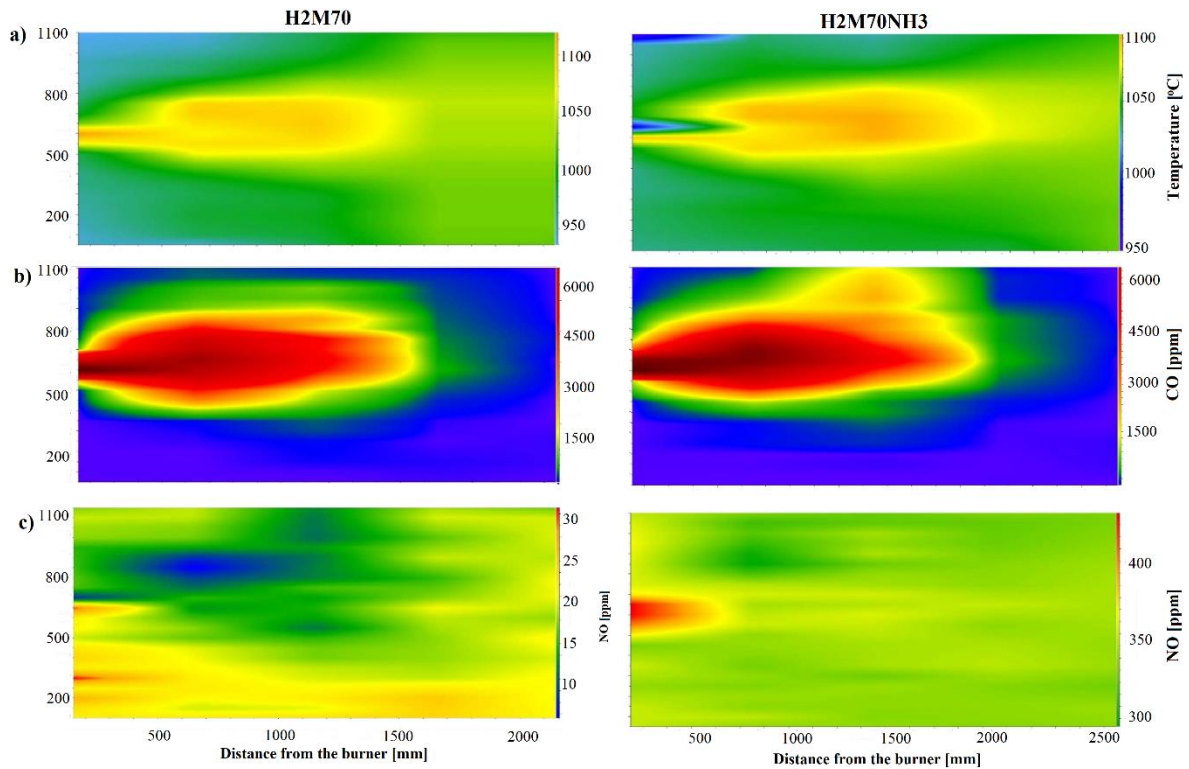


Fig. 10: Distribution of a) temperature b) carbon monoxide c) nitrogen oxide NO for H2M70 and H2M70NH3 fuels ($\phi=0.85$).

In the distribution of CO levels inside the combustion chamber for the H2M70 fuel, the zone of highest levels starts near the fuel nozzle outlet. Similar to the addition of CO₂ to the combustion process, this zone is narrower when H₂ is added compared to the combustion of the M100 base fuel. The movement of the zone with the maximum CO level towards the burner is a result of the rapid hydrogen combustion, which shortens the length of the main heat release zone in the combustion chamber and reduces CO through OH radicals. This may indicate that part of the fuel burns in a short flame, similar to conventional combustion with a high value of hydrogen laminar combustion velocity, while the remaining part undergoes the volumetric nature of combustion in accordance with the HiTAC technology.

The zone of NO reduction is located near the burner wall, which is also an area where a zone with low NO formation intensity was observed for the M100 fuel. A very similar temperature profile was obtained for H2M70NH3 fuel compared to the analysis of H2M70 fuel. It can be concluded that the addition of ammonia does not significantly affect the location of the increased temperature zone or the maximum temperatures when H₂ is added to the main fuel. Only a localised decrease in temperature near the fuel nozzle outlet was observed, which may be attributed to the lower reaction rate of ammonia oxidation in the fuel mixture. The shape and distribution of CO inside the chamber are similar to fuel without the addition of NH₃.

1
2
3
4
5
6
7
8
9
10
11
12
13
14
15
16
17
18
19
20
21
22
23
24
25
26
27
28
29
30
31
32
33
34
35
36
37
38
39
40
41
42
43
44
45
46
47
48
49
50
51
52
53
54
55
56
57
58
59
60
61
62
63
64
65

The analysis of nitrogen oxide distribution concludes that the main area of nitrogen oxide formation is at the fuel inlet of the combustion chamber. This region is characterised by a low temperature, indicating the formation of NO through the fuel and prompt mechanism. No significant areas of increased concentration or NO reduction were noticed in the remaining parts of the combustion chamber.

It is worth mentioning that, in the majority of tests conducted with various fuels, the proportion of CO in the exhaust gas remains below 100 ppm when $\phi = 0.95$. However, at $\phi = 0.85$ and 0.75 , the highest observed level of CO in the exhaust gas was 20 ppm.

4. Conclusions

Based on the conducted experiments, the following conclusions can be drawn:

- The conversion of ammonia to nitrogen oxides (NO) under combustion conditions strongly depends on the amount of air supplied for the fuel oxidation reaction.
- The lowest conversion of ammonia to nitrogen oxides was observed when the combustion process was conducted with a small excess of air in the combustion reaction zone.
- The addition of CO₂ under high-temperature conditions significantly affects the heat release characteristics in the chamber and the kinetics of the combustion reaction.
- The conversion of ammonia to NO is non-linear and decreases with an increase in the proportion of CO₂ in the fuel. In addition, a phenomenon occurs under conditions of high equivalence ratio and high CO₂ content in the fuel, leading to an increase in NO content in the flue gas.
- The fuel mechanism plays a dominant role in the formation of nitrogen oxides for fuels with ammonia content.
- Local temperature levels in the combustion chamber have no direct impact on the formation of NO_x.
- The different fuel compositions supplied to the combustion chamber do not result in significant changes in the distribution and formation of high temperature gradients areas within the test chamber.
- The most beneficial additive in terms of nitrogen oxide emissions was carbon dioxide. At $\phi=0.95$ for its mixture 5%NH₃ and 50%CH₄ (BioM50 fuel) allowed to achieve NO level below 100ppmv.
- The study results demonstrate that ammonia as additive to decarbonized fuels up to 5%vol. level, can be effectively combusted in industrial furnaces avoiding its transfer to fuel NO according to fuel mechanism.

Acknowledgements

Cardiff University authors gratefully acknowledge the support from the ESPRC through the program SAFE AGT (EP/T009314/1). Information on the data underpinning the results presented here, including how to access them, can be found in the Cardiff University data catalogue at <http://orca.cf.ac.uk/XXXXX>.

Data Availability

All data is provided in full in the results section of this paper.

References

- 1
2
3 [1] McGee M. Global Warming Update. 2022 [cited 2022 17.05]; Available from:
4 <https://www.co2.earth/global-warming-update>. n.d.
5
6
7 [2] IPCC I. Summary for Policymakers” in Global warming of 1.5° C. An IPCC Special Report on
8 the impacts of global warming of 1.5° C above pre-industrial levels and related global
9 greenhouse gas emission pathways, in the context of strengthening the global response t. 2018.
10
11
12 [3] Salehi J, Namvar A, Gazijahani FS, Shafie-khah M, Catalão JPS. Effect of power-to-gas
13 technology in energy hub optimal operation and gas network congestion reduction. *Energy*
14 2022;240:122835. <https://doi.org/https://doi.org/10.1016/j.energy.2021.122835>.
15
16
17 [4] Götz M, Lefebvre J, Mörs F, McDaniel Koch A, Graf F, Bajohr S, et al. Renewable Power-to-
18 Gas: A technological and economic review. *Renew Energy* 2016;85:1371–90.
19 <https://doi.org/10.1016/j.renene.2015.07.066>.
20
21
22 [5] Wang B, Li T, Gong F, Othman MHD, Xiao R. Ammonia as a green energy carrier:
23 Electrochemical synthesis and direct ammonia fuel cell - a comprehensive review. *Fuel Process*
24 *Technol* 2022;235:107380. <https://doi.org/https://doi.org/10.1016/j.fuproc.2022.107380>.
25
26
27 [6] Scheller F, Wald S, Kondziella H, Gunkel PA, Bruckner T, Keles D. Future role and economic
28 benefits of hydrogen and synthetic energy carriers in Germany: a review of long-term energy
29 scenarios. *Sustain Energy Technol Assessments* 2023;56:103037.
30 <https://doi.org/10.1016/J.SETA.2023.103037>.
31
32
33 [7] Duczowska A, Kulińska E, Plutecki Z, Rut J. Sustainable Agro-Biomass Market for Urban
34 Heating Using Centralized District Heating System. *Energies* 2022;15.
35 <https://doi.org/10.3390/en15124268>.
36
37
38 [8] Hosseini SE, Wahid MA, Abuelnuor AAA. Biogas flameless combustion: A review. *Appl*
39 *Mech Mater* 2013;388:273–9. <https://doi.org/10.4028/www.scientific.net/AMM.388.273>.
40
41
42 [9] Kojima H, Nagasawa K, Todoroki N, Ito Y, Matsui T, Nakajima R. Influence of renewable
43 energy power fluctuations on water electrolysis for green hydrogen production. *Int J Hydrogen*
44 *Energy* 2023;48:4572–93. <https://doi.org/https://doi.org/10.1016/j.ijhydene.2022.11.018>.
45
46
47 [10] Valera-Medina A, Xiao H, Owen-Jones M, David WIF, Bowen PJ. Ammonia for power. *Prog*
48 *Energy Combust Sci* 2018;69:63–102. <https://doi.org/10.1016/J.PECS.2018.07.001>.
49
50
51 [11] Wüning JA, Wüning JG. Flameless oxidation to reduce thermal no-formation. *Prog Energy*
52 *Combust Sci* 1997;23:81–94. [https://doi.org/10.1016/S0360-1285\(97\)00006-3](https://doi.org/10.1016/S0360-1285(97)00006-3).
53
54
55 [12] Weber R, Gupta AK, Mochida S. High temperature air combustion (HiTAC): How it all
56
57
58
59
60
61
62
63
64
65

started for applications in industrial furnaces and future prospects Preheated air. *Appl Energy* 2020;278:115551. <https://doi.org/10.1016/j.apenergy.2020.115551>.

- [13] Tsuji H, Gupta AK, Hasegawa T, Katsuki M, Kishimoto K, Morita M. *High Temperature Air Combustion From Energy Conservation to Pollution Reduction*. CRC Press. Boca Raton: 2002. <https://doi.org/https://doi.org/10.1201/9781420041033>.
- [14] Szewczyk D, Jankowski R, Ślefarski R, Chmielewski J. Experimental study of the combustion process of gaseous fuels containing nitrogen compounds with the use of new, low-emission Zonal Volumetric Combustion technology. *Energy* 2015;92. <https://doi.org/10.1016/j.energy.2015.04.063>.
- [15] Szewczyk D, Skotnicki P. Zalety technologii wysokotemperaturowego spalania objętościowego HiTAC w procesach utylizacji gazów odpadowych i niskokalorycznych. *Piece Przem Kotły* 2012;7–8:31–9.
- [16] Mochida S, Hasegawa T. High temperature air combustion burner system for small size heating equipment. *Proc Int Jt Power Gener Conf* 2001;1:223–9.
- [17] He J, Shi L, Tian H, Wang X, Zhang Y, Zhang M, et al. Control strategy for a CO₂-based combined cooling and power generation system based on heat source and cold sink fluctuations. *Energy* 2022;257:124716. <https://doi.org/https://doi.org/10.1016/j.energy.2022.124716>.
- [18] Qin W, Egolfopoulos FN, Tsotsis TT. Fundamental and environmental aspects of landfill gas utilization for power generation 2001;82:157–72.
- [19] Erete JI, Hughes KJ, Ma L, Fairweather M, Pourkashanian M, Williams A. Effect of CO₂ dilution on the structure and emissions from turbulent, non-premixed methane air jet flames. *J Energy Inst* 2016. <https://doi.org/10.1016/j.joei.2016.02.004>.
- [20] Jia H, Zou C, Lu L, Zheng H, Qian X, Yao H. Ignition of CH₄ intensely diluted with N₂ and CO₂ versus hot air in a counter flow jets. *Energy* 2018;165:315–25. <https://doi.org/10.1016/j.energy.2018.09.081>.
- [21] Yang J, Gong Y, Guo Q, Zhu H, He L, Yu G. Dilution effects of N₂ and CO₂ on flame structure and reaction characteristics in CH₄/O₂ flames. *Exp Therm Fluid Sci* 2019;108:16–24. <https://doi.org/https://doi.org/10.1016/j.expthermflusci.2019.06.003>.
- [22] Bazooyar B, Darabkhani HG. The design strategy and testing of an efficient microgas turbine combustor for biogas fuel. *Fuel* 2021;294:120535. <https://doi.org/10.1016/j.fuel.2021.120535>.
- [23] Guiberti TF, Durox D, Schuller T. Flame chemiluminescence from CO₂ and N₂ diluted laminar CH₄/air premixed flames 2017;181:110–22.

<https://doi.org/10.1016/j.combustflame.2017.01.032>.

- 1
2 [24] Liu F, Guo H, Smallwood GJ. The chemical effect of CO₂ replacement of N₂ in air on the
3 burning velocity of CH₄ and H₂ premixed flames. *Combust Flame* 2003;133:495–7.
4 [https://doi.org/10.1016/S0010-2180\(03\)00019-1](https://doi.org/10.1016/S0010-2180(03)00019-1).
5
6
7 [25] Zhang J, Mi J, Li P, Wang F, Dally BB. Moderate or intense low-oxygen dilution combustion
8 of methane diluted by CO₂ and N₂. *Energy and Fuels* 2015;29:4576–85.
9 <https://doi.org/10.1021/acs.energyfuels.5b00511>.
10
11
12 [26] Caoz, Tong Z. Effects of CO₂ Dilution on Methane Ignition in Moderate or Intense Low-
13 oxygen Dilution (MILD) Combustion: A Numerical Study. *Chinese J Chem Eng*
14 2012;20:701–9. [https://doi.org/10.1016/S1004-9541\(11\)60238-3](https://doi.org/10.1016/S1004-9541(11)60238-3).
15
16
17 [27] Colorado AF, Herrera BA, Amell AA. Performance of a Flameless combustion furnace using
18 biogas and natural gas. *Bioresour Technol* 2010;101:2443–9.
19 <https://doi.org/10.1016/j.biortech.2009.11.003>.
20
21
22 [28] Mameri A, Tabet F, Hadeif A, Mhidi B, Bouaghi O El. ScienceDirect MILD combustion of
23 hydrogenated biogas under several operating conditions in an opposed jet configuration. *Int J*
24 *Hydrogen Energy* 2017;43:3566–76. <https://doi.org/10.1016/j.ijhydene.2017.04.273>.
25
26
27 [29] Zeldovich YB. The Oxidation of Nitrogen in Combustion and Explosions. *Sel Work Yakov*
28 *Borisovich Zeldovich, Vol I* 2015;216:364–403. <https://doi.org/10.1515/9781400862979.364>.
29
30
31 [30] Ferrarotti M, De Paepe W, Parente A. Reactive structures and NO_x emissions of
32 methane/hydrogen mixtures in flameless combustion. *Int J Hydrogen Energy* 2021;46:34018–
33 45. <https://doi.org/10.1016/j.ijhydene.2021.07.161>.
34
35
36 [31] Escalante Soberanis MA, Fernandez AM. A review on the technical adaptations for internal
37 combustion engines to operate with gas/hydrogen mixtures. *Int J Hydrogen Energy*
38 2010;35:12134–40. <https://doi.org/10.1016/j.ijhydene.2009.09.070>.
39
40
41 [32] Cavigiolo A, Galbiati MA, Effuggi A, Gelosa D, Rota R. Mild combustion in a laboratory-
42 scale apparatus. *Combust Sci Technol* 2003;175:1347–67.
43 <https://doi.org/10.1080/00102200302356>.
44
45
46 [33] Celtek MS. Flameless combustion investigation of CH₄/H₂ in the laboratory-scaled furnace.
47 *Int J Hydrogen Energy* 2020;45:35208–22. <https://doi.org/10.1016/j.ijhydene.2020.05.233>.
48
49
50 [34] Smith GP, Golden DM, Frenklach M, Moriarty NW, Eiteneer B, Goldenberg M, Bowman TC,
51 Hanson RK, Song S, Gardiner WC, LissianskicVV, Qin Z. GRI-Mech 3.0
52 http://www.me.berkeley.edu/gri_mech/
53
54
55 [35] Ayoub M, Rottier C, Carpentier S, Villermaux C, Boukhalifa AM, Honoré D. An experimental
56
57
58
59
60
61
62
63
64
65

study of mild flameless combustion of methane/hydrogen mixtures. *Int J Hydrogen Energy* 2012;37:6912–21. <https://doi.org/10.1016/j.ijhydene.2012.01.018>.

- [36] Cano Ardila FE, Obando Arbeláez JE, Amell Arrieta AA. Emissions and dynamic stability of the flameless combustion regime using hydrogen blends with natural gas. *Int J Hydrogen Energy* 2021;46:1246–58. <https://doi.org/10.1016/j.ijhydene.2020.09.236>.
- [37] Goodwin DG, Moffat HK, Speth RL. *Cantera: An Object-Oriented Software Toolkit For Chemical Kinetics, Thermodynamics And Transport Processes*. Version 2.3.0 2017. <https://doi.org/10.5281/ZENODO.170284>.
- [38] Mendiara T, Glarborg P. Ammonia chemistry in oxy-fuel combustion of methane. *Combust Flame* 2009;156:1937–49. <https://doi.org/10.1016/j.combustflame.2009.07.006>.
- [39] Chai WS, Bao Y, Jin P, Tang G, Zhou L. A review on ammonia , ammonia-hydrogen and ammonia-methane fuels. *Renew Sustain Energy Rev* 2021;147:111254. <https://doi.org/10.1016/j.rser.2021.111254>.
- [40] Gurz M, Baltacioglu E, Hames Y, Kaya K. The meeting of hydrogen and automotive: A review. *Int J Hydrogen Energy* 2017;42:23334–46. <https://doi.org/10.1016/j.ijhydene.2017.02.124>.
- [41] Ahrenfeldt J, Thomsen TP, Henriksen U, Clausen LR. Biomass gasification cogeneration - A review of state of the art technology and near future perspectives. *Appl Therm Eng* 2013;50:1407–17. <https://doi.org/10.1016/j.applthermaleng.2011.12.040>.
- [42] Szewczyk D, Ślefarski R, Jankowski R. Analysis of the combustion process of syngas fuels containing high hydrocarbons and nitrogen compounds in Zonal Volumetric Combustion technology. *Energy* 2017;121:716–25. <https://doi.org/10.1016/j.energy.2017.01.040>.
- [43] Slefarski R, Czyzewski P, Golebiewski M. Experimental Study on Combustion of CH₄/NH₃ Fuel Blends in an Industrial Furnace Operated in Flameless Conditions. *Therm Sci* 2020;24:3625–36235. <https://doi.org/10.2298/TSCI200401282S>.
- [44] Miller JA, Smooke MD, Green RM, Kee RJ. Kinetic Modeling of the Oxidation of Ammonia in Flames. *Combust Sci Technol* 1983;34:149–76. <https://doi.org/10.1080/00102208308923691>.

1
2
3
4
5
6
7
8
9
10
11
12
13
14
15
16
17
18
19
20
21
22
23
24
25
26
27
28
29
30
31
32
33
34
35
36
37
38
39
40
41
42
43
44
45
46
47
48
49
50
51
52
53
54
55
56
57
58
59
60
61
62
63
64
65

CRedit author statement

Pawel Czyzewski: Conceptualization, Methodology, Software, Formal analysis, Investigation, Writing – original Draft. **Rafal Slefarski:** Methodology, Writing - Review & Editing, Supervision, Resources. **Michal Golebiewski:** Conceptualization, Investigation, Validation. **Mohammad Alnajideen:** Validation, Writing - Review & Editing, Visualization. **Agustin Valera-Medina:** Writing - Review & Editing, Visualization